Dalton Transactions

Accepted Manuscript

This article can be cited before page numbers have been issued, to do this please use: A. Kasprzak, M. Bystrzejewski and M. Popawska, *Dalton Trans.*, 2018, DOI: 10.1039/C8DT00677F.

ROYAL SOCIETY OF CHEMISTRY

rsc.li/dalton

View Article Online
DOI: 10.1039/C8DT00677F

Sulfonated carbon-encapsulated iron nanoparticles as efficient magnetic nanocatalyst for highly selective synthesis of benzimidazoles

Artur Kasprzak[a]*, Michał Bystrzejewski[b], Magdalena Poplawska[a]

*e-mail: akasprzak@ch.pw.edu.pl

[a] Faculty of Chemistry, Warsaw University of Technology, 00-664 Warsaw, Poland

[b] Faculty of Chemistry, University of Warsaw, 02-093 Warsaw, Poland

Abstract

Surface functionalized carbon-encapsulated iron nanoparticles (CEINs) were found to be a magnetic nanocatalyst for the efficient and highly selective synthesis of benzimidazoles. CEINs were covalently decorated with carboxyl or sulfonyl groups and their catalytic activity was examined. Carboxyl-modified CEINs were obtained via the radical or oxidative treatment, whilst the sulfonated CEINs were obtained using one-step diazotization approach with sulfanilic acid and isoamyl nitrite. The content of surface acidic groups varied between the obtained materials and was found to be the highest for sulfonyl-modified CEINs. CEINs functionalized with sulfonyl groups were the most efficient and the most selective nanocatalyst for the synthesis of benzimidazoles. Various benzimidazoles were obtained in very high yields (92.5-97.0%). Both metallocene, aliphatic, heterocyclic and aromatic aldehydes substituted with different functional groups were subjected to the synthesis process. The reaction proceeded in a short time, which varied from 25 min to 65 min depending on the aldehyde used. Additionally, the mechanism of the studied catalytic condensation applying

View Article Online
DOI: 10.1039/C8DT00677F

sulfonated CEINs as the catalyst was discussed. Importantly, the developed magnetic nanocatalysts could be easily separated from the reaction mixture using a permanent magnet. The nanocatalysts can be used up to six reaction cycles without any significant loss of its catalytic activity. This work opens up new ways for very efficient and simple synthesis of benzimidazoles – an important class organic compounds for various biomedical applications.

1. Introduction

Carbon nanomaterials, especially graphene related materials and carbon nanotubes, are considered as the most important class of solid supports for various catalytic systems.[1–3] This phenomenon is associated with the high chemical inertness of carbon materials as well as their specific physicochemical features, such as unique curvature, high surface area and high electrical conductivity. The presence of large number of conjugated rings and functional groups in the structure of carbon materials gives also a possibility of physical adsorption of various aromatic moieties via π-π-stacking or positively charged chemical individuals via electrostatic interactions.[4–6] Many methods for the non-covalent modification of carbon nanomaterials for the catalytic purposes were therefore reported. For example, to date, different types of active species were deposited on graphite and reduced graphene oxide, especially metallic catalysts, like platinum or palladium.[7–9] The application of carbon material as the solid support enables to increase the activity of the metallic particles and influences the reaction rate. These phenomena are reasoned with the fact of the (i) increased electron density on the metallic surface via π-donation, (i) oxidizing properties of carbon nanostructures, as well as (ii) adsorption of the reactant on the carbon material.[10] The adsorption of the reactant influences the reaction rate, since the contact between a metallic particle and the reactant is facilitated and the stabilization of a given intermediate on the surface of carbon support is observed.

View Article Online
DOI: 10.1039/C8DT00677F

Catalytic activity of native graphene-related materials, such as graphene oxide (GO) and carbon nanotubes (CNTs), was also demonstrated.[11–13] Noteworthy, the main issue regarding the application of GO as a catalyst is its stability. It has been demonstrated that the physicochemical properties and structure of GO might change when the material is exposed on radiation (e.g. UV), high temperature or strong acid/base conditions.[10,14,15]

The applications of magnetic carbon nanoparticles cover many areas of science, including nanomedicine[16–18], water treatment and sustainable chemistry.[19–24] Carbon-encapsulated metal nanoparticles are a class of core-shell magnetic nanomaterials.[25] A pure metallic phase which is encapsulated in graphene-like shell is responsible for relatively high magnetization of carbon-encapsulated metal nanoparticles.[26–30] Such nanostructures are also commonly termed as nanomagnets. Importantly, the carbon shell not only protects the metallic core but also enables the covalent attachment of organic ligands, e.g. via radical processes[31–33] or cycloaddition reactions[34–36]. Such phenomenon opens up avenues to apply these magnetic nanoparticles in catalysis and to develop further the field of magnetic nanocatalysis, which has been intensively studied in recent years. The magnetic nanocatalysis is of a great interest in the heterogenic catalysis because the catalyst can be easily separated from the reaction mixture when the reaction is finished. This can be reached using simple permanent magnets. For example, Stark and co-workers showed that carbon-coated cobalt nanoparticles could act as the solid matrix for covalent[37] or non-covalent[38] immobilization of palladium complexes for Suzuki-Miyamura cross-coupling. The palladium catalyst was found to be very active, as well as it can be easily separated from the reaction mixture and reused.

An emerging field of application of novel types of nanocatalysts is the synthesis of bioactive compounds. Benzimidazoles are one of the most prominent family of biologically important molecules. Benzimidazole framework is the pharmacophore for different classes of bioactive individuals, like fungicides (e.g. carbendazim), antiparasitic drugs (e.g. albendazole)

View Article Online
DOI: 10.1039/C8DT00677F

or medicines for wide range of disorders (e.g. omeprazole).[39] The synthesis of benzimidazoles is most commonly based on the condensation reaction between aromatic diamine and aldehyde. However, the yield of the process and its selectivity are relatively low. The application of a proper catalyst in this type of reaction has been widely studied. Carbon materials were reported to be a promising catalyst for the synthesis of benzimidazoles. Sharghi and co-workers have demonstrated that graphite/base or graphite/acid system can be used to obtain various benzimidazoles.[40] The synthesis yields were higher in comparison to the catalyst-free reaction. The role of graphite in this process was explained with its oxidizing properties and the presence of some carboxyl groups on its surface. In 2016, GO was reported as the acid nanocatalyst for benzimidazole synthesis.[41] The synthesis yield was reported to be between 42% and 89% and depended on the aldehyde and amine used. However, GO had to be re-oxidized before the next catalytic reaction. This is because the carboxyl groups from GO were consumed in this process. Graphene oxide cannot be therefore considered as the "real" catalyst, because its structure changes after the reaction. Noteworthy, magnetic nanocatalysts, like iron oxide nanoparticles, were also applied for the synthesis of benzimidazoles.[42,43] However, the selectivity and the synthesis yield of the reaction was lower in comparison to the processes catalyzed by GO. In case of application of iron oxide nanoparticles as the catalyst for the synthesis of benzimidazoles, the nanomaterial can be relatively easily separated from the reaction mixture. Nevertheless, it was previously demonstrated that the magnetic features of iron oxides are lower in comparison to pure metallic phase.[44,45]

Herein, an efficient, simple and highly selective synthetic route to obtain various benzimidazoles using magnetic carbon-encapsulated iron nanoparticles (CEINs; Fe@C) or surface decorated CEINs as the nanocatalyst, is reported. A comparative study on the catalytic activity of (i) CEINs, (ii) carboxyl-modified CEINs and (iii) sulfonyl-modified CEINs, is presented. An efficient method for the decoration of CEINs with sulfonyl groups, is also

View Article Online
DOI: 10.1039/C8DT00677F

demonstrated. It is also shown that CEINs-based nanocatalyst can be easily separated from the reaction mixture because of its strong ferromagnetic properties. The recyclability study and proposed reaction mechanism are also presented.

2. Experimental section

2.1 Materials and methods

Ferrocenecarboxaldehyde (98%), 4-nitrobenzaldehyde (98%), 4-chlorobenzaldehyde (97), heptanal (95%), 4-tert-butylbenzaldehyde (97%), 4-(dimethylamino)benzaldehyde (98%), 4-hydroxybenzaldehyde (98%), 4-carboxybenzaldehyde (97%), 1,2-phenylenediamine (99.5%) were purchased from Sigma-Aldrich. (E)-Cinnamaldehyde (>95), 4-tolualdehyde (97%), 2-pyridinecarboxaldehyde (98%), 1-pyrenecarboxaldehyde (99%) were purchased from Acros Organics. Sulfanilic acid (99%) was purchased from Fluorochem. Benzaldehyde (>98%), ethyl acetate (>99%), hexane (>99%), dichloromethane (>99.5%), dietyhlether (>99.5%), methanol (>99%), ethanol (99.8%) were purchased from Avantor Performance Materials Poland S.A. All reagents were used as received without purification.

Thin layer chromatography (TLC; silica gel 60 matrix) plates and preparative thin layer chromatography (PTLC; silica gel 60 matrix, layer thickness 2000 μm) plates were purchased from Merck.

Sonication was performed using a Bandelin Sonorex RK 100 H ultrasonic probe with a temperature control (ultrasonic peak output/HF power: 320W/80W; 35 kHz).

Thermogravimetric analysis (TGA) was performed with a TA Q-50 instrument under nitrogen atmosphere with the heating rate of 10 °C·min^{-1}.

Fourier transformation infrared (FT-IR) spectra were recorded in a transmission mode with a Thermo Scientific Nicolet iS5 spectrometer with the spectral resolution of 4cm^{-1}. The samples were mixed with KBr and pressed in a form of pellets.

View Article Online
DOI: 10.1039/C8DT00677F

^{1}H NMR and ^{13}C NMR spectra were recorded on a Varian NMR System spectrometer (500 MHz, 125 MHz) in DMSO-d_6 with calibration on the residual peak 2.50 ppm and 39.5 ppm, for ^{1}H NMR and ^{13}C NMR, respectively. The MestRe-C 2.0 software was used for the simulation of NMR spectra (*MestRe-C NMR Data Processing Made Easy 4.9.9.6, 1996–2006, courtesy F.J. Sardina, Universidad de Santiago de Compostela, Spain*).

2.2 Synthesis of the nanocatalysts

Synthesis of Fe@C ***(NANOCAT-G1)****, Fe@C-COOH* ***(NANOCAT-G2)*** *and Fe@C-(CH)$_2$-COOH* ***(NANOCAT-G3)***

Carbon-encapsulated iron nanoparticles (CEINs; Fe@C) were synthesized using the carbon-arc route. The protocol is described in detail elsewhere.[25] Fe@C-COOH were obtained via the oxidative treatment with nitric acid and sulfuric acid, whilst Fe@C-(CH)$_2$-COOH was obtained using a radical process with succinic acid acyl peroxide.[31] The reaction paths are presented in **Scheme 1a-b**. Hereafter, these materials are referred as **NANOCAT-G1**, **NANOCAT-G2** and **NANOCAT-G3**, for Fe@C, Fe@C-COOH and Fe@C-(CH)$_2$-COOH, respectively.

Synthesis of Fe@C-Ph-SO$_3$H ***(NANOCAT-G4)***

Isoamyl nitrite was synthesized using the previously reported method.[46] **NANOCAT-G4** was obtained using a diazotization approach. The reaction scheme is presented in **Scheme 1c**. Prior to the functionalization, Fe@C (200 mg) were sonicated in o-dichlorobenzene (100 mL) for 1 h. Sulfanilic acid (2.7712 g, 16.0 mmol) and isoamyl nitrite (2.6 mL, 2.2672 g, 32 mmol, 200 mol%) were then added. The reaction mixture was sonicated at 70 °C under argon atmosphere for 9 h followed by heating at 70 °C overnight. Then, the reaction mixture was once again sonicated at 70 °C for 9 h and heated at 70 °C overnight. The suspension

View Article Online
DOI: 10.1039/C8DT00677F

containing dispersed carbon material was filtrated off and washed with acetone (20 mL) and ethanol (100 mL). The resultant carbon material was suspended in 100 mL of 1M NaOH (100 mL), sonicated for 1 h, filtrated off and washed with distilled water (100 mL). The as-obtained solid was suspended in 1M HCl (100 mL), sonicated for 1 h, filtrated off and washed with distilled water (100 mL). Finally, the as-obtained carbon material was washed with ethanol (20 mL) and dried in an oven at 45 °C for 24 h. About 225 mg of Fe@C-Ph-SO_3H (**NANOCAT-G4)** was obtained.

NANOCAT-G4 (Fe@C-Ph-SO_3H):

FT-IR (KBr): υ = 1630, 1600, 1496, 1520, 1160, 1125, 1036, 1010, 830, 680, 580 cm^{-1}

TGA (content of introduced organic moiety): 28.0 wt%

Content of SO_3H groups (back titration)[47]: 2.11 mmol/g

View Article Online
DOI: 10.1039/C8DT00677F

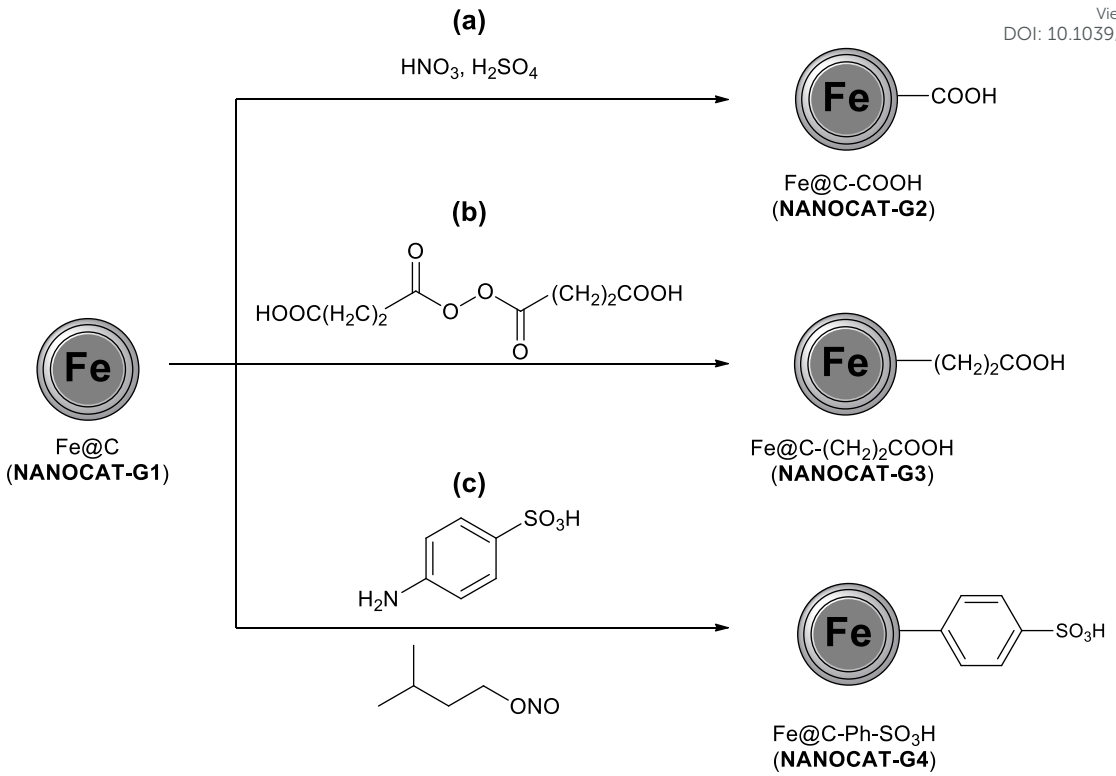

Scheme 1. Structure of Fe@C (**NANOCAT-G1**) and synthesis of **(a)** Fe@C-COOH **(NANOCAT-G2)**, **(b)** Fe@C-$(CH)_2$-COOH **(NANOCAT-G3)** and **(c)** Fe@C-Ph-SO_3H (**NANOCAT-G4)**

2.3 General procedure for the synthesis of benzimidazoles

The reaction path is presented in **Scheme 2**. 1,2-Phenylenediamine (43.3 mg, 0.4 mmol) was dissolved in ethanol (7 mL). The appropriate amount of the nanocatalyst (**G1**, **2**, **3** or **4**) was then added and the mixture was sonicated at 40 °C for 15 min. Aldehyde (**1-13**, 0.4 mmol, 100 mol%) was subsequentially added and the reaction mixture was sonicated at 40 °C for appropriate time (see data in **Table 4**). The progress of the reaction was monitored by TLC using an appropriate solvent system as the mobile phase. After the completion of the reaction, the catalyst was separated from the reaction mixture either using a magnet. The supernatant was separated from the catalyst. The carbon material was then sonicated with ethanol (7 mL) for 15 min and once again the supernatant was collected. In case of 2-(1-

View Article Online
DOI: 10.1039/C8DT00677F

pyrenyl)benzimidazole (**7**) washing of the catalyst was repeated twice. The collected organic layers were concentrated using a rotary evaporator to afford a crude product. The pure product was isolated by means of PTLC with the same solvent system as used in TLC. The reaction yield was calculated based on the mass of the purified product. The structure of the product was confirmed by ^{1}H NMR, ^{13}C NMR and FT-IR. The spectral data for the obtained benzimidazoles are consistent with the literature. The structures of all obtained benzimidazoles (**1-13**) are presented in **Table 4**.

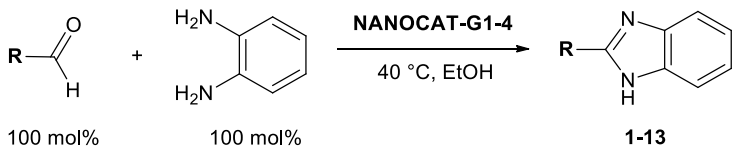

Scheme 2. Synthesis of benzimidazoles using the herein developed nanocatalysts. Structures of **NANOCAT-G1-4** are presented in scheme 1. For the structure of the benzimidazoles obtained and reactions conditions, see **Table 4**

2-phenylbenzimidazole (**1**)

white solid, yield: 95.0%

R_f (30%v/v AcOEt/hex) = 0.76

^{1}H NMR (DMSO-d$_6$, 500 MHz): δ_H 12.92 (bs, 1H), 8.20-8.18 (m, 2H), 7.67-7.49 (m, 5H), 7.21-7.20 (m, 2H)

^{13}C NMR (DMSO-d$_6$, 125 MHz): δ_C 151.2, 143.8, 135.0, 130.1, 129.8, 126.4, 122.5, 121.6, 118.8, 111.3

FT-IR (KBr): υ = 2920, 2780, 2695, 1595, 1535, 1435, 1395, 1275, 1120, 960, 750, 700 cm^{-1}

View Article Online
DOI: 10.1039/C8DT00677F

2-(4-tolyl)benzimidazole (**2**)

light yellow solid, yield: 96.5%

R_f (30%v/v AcOEt/hex) = 0.46

^{1}H NMR (DMSO-d$_6$, 500 MHz): δ_H 12.81 (bs, 1H), 8.06-8.06 (m, 2H), 7.64-7.51 (m, 2H), 7.36-7.35 (m, 2H), 7.19-7.18 (m, 2H), 2.38 (s, 3H)

^{13}C NMR (DMSO-d$_6$, 125 MHz): δ_C 151.2, 143.6, 139.3, 134.7, 129.3, 126.2, 121.1, 121.3, 118.5, 111.0, 20.8

FT-IR (KBr): υ = 2920, 2860, 2750, 1585, 1495, 1430, 1280, 1220, 960, 820, 750, 540 cm^{-1}

2-(4-tert-butylphenyl)benzimidazole (**3**)

light yellow solid, yield: 95.0%

R_f (30%v/v AcOEt/hex) = 0.59

^{1}H NMR (DMSO-d$_6$, 500 MHz): δ_H 12.81 (bs, 1H), 8.10-8.08 (m, 2H), 7.64-7.49 (m, 4H), 7.17-7.16 (m, 2H), 1.31 (s, 9H)

^{13}C NMR (DMSO-d$_6$, 125 MHz): δ_C 152.5, 151.2, 143.8, 134.9, 127.4, 126.2, 125.7, 122.3, 121.5, 118.7, 111.1, 34.6, 30.9

FT-IR (KBr): υ = 2935, 2785, 2700, 1620, 1565, 1420, 1330, 1270, 1220, 1000, 820, 750, 490 cm^{-1}

*2-(4-chlorophenyl)benzimidazole (**4**)*

light yellow solid, yield: 96.5%

R_f (30%v/v AcOEt/hex) = 0.51

^{1}H NMR (DMSO-d$_6$, 500 MHz): δ_H 13.00 (bs, 1H), 8.20-8.18 (m, 2H), 7.64-7.60 (m, 2H), 7.22-7.21 (m, 2H)

View Article Online
DOI: 10.1039/C8DT00677F

^{13}C NMR (DMSO-d$_6$, 125 MHz): δ_C 150.1, 134.5, 130.8, 129.7, 129.0, 128.8, 128.1, 122.7, 121.8, 118.9

FT-IR (KBr): υ = 2925, 2855, 2740, 1605, 1430, 1325, 1270, 1090, 965, 835, 745, 540 cm^{-1}

*2-(4-hydroxyphenyl)benzimidazole (**5**)*

light orange solid, yield: 96.5%

R_f (30%v/v hex/AcOEt) = 0.53

^{1}H NMR (DMSO-d$_6$, 500 MHz): δ_H 12.64 (bs, 1H), 9.98 (bs, 1H), 8.01-8.00 (m, 2H), 7.59-7.48 (m, 2H), 7.15-7.14 (m, 2H), 6.92-6.91 (m, 2H)

^{13}C NMR (DMSO-d$_6$, 125 MHz): δ_C 158.9, 151.6, 135.7, 134.8, 134.7, 130.4, 127.9, 121.6, 121.0, 118.1, 115.5, 110.7

FT-IR (KBr): υ = 3085, 2925, 2810, 2680, 1620, 1460, 1390, 1275, 1180, 1020, 840, 755, 520 cm^{-1}

*2-(4-dimethylaminophenyl)benzimidazole (**6**)*

pale yellow solid, yield: 94.5%

R_f (30%v/v hex/AcOEt) = 0.65

^{1}H NMR (DMSO-d$_6$, 500 MHz): δ_H 12.53 (bs, 1H), 8.01-7.99 (m, 2H), 7.55-7.45 (m, 2H), 7.13-7.11 (m, 2H), 6.84-6.82 (m, 2H), 2.99 (s, 6H)

^{13}C NMR (DMSO-d$_6$, 125 MHz): δ_C 152.2, 151.2, 129.8, 127.5, 121.4, 121.2, 121.1, 118.0, 117.4, 112.4, 111.8, 110.6, 41.1

FT-IR (KBr): υ = 2920, 2860, 2785, 1610, 1500, 1435, 1370, 1280, 1090, 940, 745, 540 cm^{-1}

*2-(1-pyrenyl)benzimidazole (**7**)*

yellow solid, yield: 95.0%

View Article Online
DOI: 10.1039/C8DT00677F

R_f (30%v/v AcOEt/hex) = 0.49

^{1}H NMR (DMSO-d_6, 500 MHz): δ_H 13.12 (bs, 1H), 9.50-9.49 (m, 2H), 8.56-8.49 (m, 2H), 8.39-8.27 (m, 5H), 8.16-8.10 (m, 2H), 7.86-7.84 (m, 1H), 7.65-7.63 (m, 1H), 7.31-7.28 (m, 2H)

^{13}C NMR (DMSO-d_6, 125 MHz): δ_C 151.1, 144.1, 134.7, 131.6, 130.8, 130.3, 128.6, 128.3, 127.3, 126.6, 125.9, 125.6, 124.8, 124.3, 123.7, 122.7, 121.7, 121.6, 119.1, 111.4

FT-IR (KBr): υ = 3020, 2910, 2845, 1580, 1545, 1425, 1360, 1270, 955, 840, 745 cm^{-1}

*2-(ferrocenyl)benzimidazole (**8**)*

orange solid, yield: 92.5%

R_f (50%v/v DCM/ether) = 0.76

^{1}H NMR (DMSO-d_6, 500 MHz): δ_H 12.36 (bs, 1H), 7.54-7.44 (m, 2H), 7.13-7.12 (m, 2H), 5.04 (s, 2H), 4.47 (s, 2H), 4.10 (s, 5H)

^{13}C NMR (DMSO-d_6, 125 MHz): δ_C 152.7, 143.8,134.5, 121.3, 117.7, 110.3, 74.1, 69.1, 67.1

FT-IR (KBr): υ = 2935, 2800, 2695, 1615, 1565, 1425, 1335, 1270, 1215, 1010, 820, 755, 475 cm^{-1}

*2-(4-nitrophenyl)benzimidazole (**9**)*

yellow solid, yield: 94.5%

R_f (30%v/v AcOEt/hex) = 0.42

^{1}H NMR (DMSO-d_6, 500 MHz): δ_H 13.29 (bs, 1H), 8.41-8.40 (m, 4H), 7.66-7.64 (m, 2H), 7.27-7.26 (m, 2H)

^{13}C NMR (DMSO-d_6, 125 MHz): δ_C 149.0, 147.8, 136.0, 127.4, 124.3, 123.0, 122.9, 122.8

FT-IR (KBr): υ = 2920, 2860, 2735, 1605, 1515, 1430, 1340, 1275, 1100, 970, 860, 745 cm^{-1}

View Article Online
DOI: 10.1039/C8DT00677F

*2-(4-carboxyphenyl)benzimidazole (**10**)*

yellow solid, yield: 95.0%

R_f (10%v/v MeOH/DCM) = 0.50

^{1}H NMR (DMSO-d$_6$, 500 MHz): δ_H 13.09 (bs, 2H), 8.30-8.29 (m, 2H), 8.11-8.10 (m, 2H), 7.64-7.62 (m, 2H), 7.24-7.23 (m, 2H)

^{13}C NMR (DMSO-d$_6$, 125 MHz): δ_C 166.9, 150.2, 133.8, 131.8, 129.9, 129.3, 126.4, 122.7, 122.5, 122.3, 121,0

FT-IR (KBr): υ = 3180, 2920, 2850, 1695, 1615, 1435, 1230, 1125, 1030, 860, 755, 690 cm^{-1}

*2-(2-pyridyl)benzimidazole (**11**)*

yellow solid, yield: 95.5%

R_f (10%v/v MeOH/DCM) = 0.70

^{1}H NMR (DMSO-d$_6$, 500 MHz): δ_H 13.09 (bs, 1H), 8.74-8.72 (m, 1H), 8.34-8.32 (m, 1H), 8.01-7.98 (m, 1H), 7.71-7.70 (m, 1H), 7.55-7.51 (m, 2H), 7.26-7.20 (m, 2H)

^{13}C NMR (DMSO-d$_6$, 125 MHz): δ_C 150.7, 149.3, 148.5, 143.8, 137.5, 134.9,124.6, 123.1, 121.8, 121.4, 119.2, 112.0

FT-IR (KBr): υ = 3055, 2960, 2845, 1595, 1450, 1405, 1305, 1280, 1125, 1000, 745, 710 cm^{-1}

*(E)-2-styrylbenzimidazole (**12**)*

light yellow solid, yield: 96.5%

R_f (40%v/v AcOEt/hex) = 0.62

^{1}H NMR (DMSO-d$_6$, 500 MHz): δ_H 12.62 (bs, 1H), 7.68-7.65 (m, 4H), 7.45-7.42 (m, 3H), 7.37-7.34 (m, 2H), 7.24 (m, 1H), 7.21 (m, 1H)

^{13}C NMR (DMSO-d$_6$, 125 MHz): δ_C 150.09, 144.0, 135.7, 134.2, 128.9, 128.8, 127.0, 122.5, 121.5, 118.6, 118.5, 117.7, 111.0

View Article Online
DOI: 10.1039/C8DT00677F

FT-IR (KBr): υ = 2920, 2730, 1630, 1520, 1410, 1275, 1230, 1030, 960, 745, 515 cm^{-1}

*2-hexylbenzimidazole (**13**)*

light yellow solid, yield: 97.0%

R_f (30%v/v AcOEt/hex) = 0.43

^{1}H NMR (DMSO-d_6, 500 MHz): δ_H 12.14 (bs, 1H), 7.45-7.43 (m, 2H), 7.10-7.08 (m, 2H), 2.80-2.77 (t, *J* = 7.6 Hz, 2H), 1.75-1.73 (m, 2H), 1.28-1.27 (m, 6H), 0.86-0.83 (t, *J* = 7.1 Hz, 3H)

^{13}C NMR (DMSO-d_6, 125 MHz): δ_C 155.1, 121.0, 120.9, 30.9, 28.5, 28.3, 27.5, 21.9

FT-IR (KBr): υ = 2930, 2850, 2735, 2680, 1540, 1430, 1270, 1020, 935, 740 cm^{-1}

2.4 Recyclability study on **NANOCAT-G4**

After washing with ethanol, **NANOCAT-G4** used in the synthesis of benzimidazoles (2.3) was dried in 45 °C for 24 h. The resultant carbon material was subjected to the reaction between 1,2-phenylenediamine (0.4 mmol) and benzaldehyde (0.4 mmol). The procedure was the same as described in subsection 2.3. After the reaction, **NANOCAT-G4** was washed with ethanol (2x7mL), dried in 45 °C for 24 h and once again subjected to the condensation of 1,2-phenylenediamine (0.4 mmol) and benzaldehyde (0.4 mmol). The evaluated yield of the reaction indicated the catalytic activity of the as-regenerated material.

3 Results and discussion

The herein developed method for the synthesis of **NANOCAT-G4** employed the one-step diazotization approach (**Scheme 1c**). The method for the synthesis of **NANOCAT-G4** employed the diazonium salt generated from sulfanilic acid. Afterwards, the radical reaction

View Article Online
DOI: 10.1039/C8DT00677F

between graphene layer in CEINs and aryl radical took place. In order to provide the highest yield possible, the process was conducted in organic solvent (o-dichlorobenzene). The diazonium salt was generated using the isoamyl nitrite. The success of the functionalization was confirmed by FT-IR (Fig. S1) and TGA (Fig. S2). The content of the introduced organic moiety was found to be very high (28.0 wt%) and this value corresponded to high surface acidity (2.11 mmol/g). Importantly, the evaluated surface acidity is comparable to the surface acidity of commercial cationic-exchange resigns, e.g. Amberlite (2.30-2.50 mmol/g).

3.1 Study on the catalytic activity of the obtained materials

The reaction conditions were optimized during the studies of condensation of benzaldehyde and 1,2-phenylenediamine, which was chosen as the representative process. The reaction was carried out in ethanol at 40 °C under ultrasonic irradiation. The obtained results are summarized in **Table 1**. The application of each nanocatalyst (**NANOCAT-G1-4)** enabled to increase the yield of the process. For the catalyst-free reaction, the yield was found to be 28.0% only. **NANOCAT-G4** was found to be the most efficient and the most selective nanocatalyst. 2-Phenylbenzimidazole (**1**) was obtained with a yield of 95.0% in a relative short time (50 min) and 20 mg of **NANOCAT-G4** was used only. It should be noted that such high yield of this process was not observed even when higher mass of other nanocatalyst (**NANOCAT-G1-3**) was applied. The synthesis yield changed in the following order: **NANOCAT-G1 < NANOCAT-G2 < NANOCAT-G3 < NANOCAT-G4**. This order can be reasoned when one compares the differences in the content of acidic groups (**Table 2**). The pristine CEINs (**NANOCAT-G1**) have very low total surface acidity (0.02 mmol/g) which originates from the oxygen sites that might be partially located on the graphene-like coatings.[31] In practice, for **NANOCAT-G1** the main feature that induced its catalytic activity was the oxidizing and adsorption properties, as like for other carbon materials. The content of

View Article Online
DOI: 10.1039/C8DT00677F

surface carboxylic groups for **NANOCAT-G2** and **NANOCAT-G3** was found to be 0.53 mmol/g and 1.42 mmol/g, respectively.[31] These values are lower in comparison to the sulfonated CEINs (**NANOCAT-G4**), for which the surface acidity was found to be the highest (2.11 mmol/g). Additionally, sulphonyl groups are known to be more acidic in comparison to carboxylic groups. The catalytic activity of **NANOCAT-G4** was also compared with the previously reported both carbon-based and other types of heterogeneous catalysts applied for the studied condensation of benzaldehyde and 1,2-phenyleniediamine **(Table 3)**. It was concluded that **NANOCAT-G4** provided the highest synthesis yield. Moreover, the herein developed magnetic nanocatalyst can be effectively and easily separated from the reaction mixture applying a permanent magnet. This feature is visualized in **Fig. 1**.

View Article Online
DOI: 10.1039/C8DT00677F

Table 1. Synthesis of 2-phenylbenzimidazole using different nanocatalysts (**NANOCAT-G1-4**). Reaction conditions: benzaldehyde (0.4 mmol), 1,2-phenylenediamine (0.4 mmol), ethanol (7 mL), temperature: 40 °C (ultrasonic irradiation), time: 50 min. See subsection 2.3 for experimental details

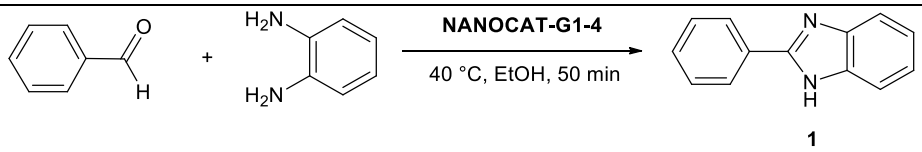

Entry	Nanocatalyst[a]	Nanocatalyst loading (mg)	Yield[b] (%)
1	none	-	28.0
2	NANOCAT-G1	10	54.0
3	NANOCAT-G1	20	58.0
4	NANOCAT-G1	30	61.0
5	NANOCAT-G1	40	60.5
6	NANOCAT-G2	10	63.0
7	NANOCAT-G2	20	68.5
8	NANOCAT-G2	30	72.0
9	NANOCAT-G2	40	73.0
10	NANOCAT-G3	10	72.0
11	NANOCAT-G3	20	81.0
12	NANOCAT-G3	30	82.0
13	NANOCAT-G3	40	81.0
14	NANOCAT-G4	10	86.0
15	**NANOCAT-G4**	20	**95.0**
16	NANOCAT-G4	30	94.5
17	NANOCAT-G4	40	94.0

[a] for the structure of the nanocatalysts see scheme 1
[b] isolated yields

View Article Online
DOI: 10.1039/C8DT00677F

Table 2. Content of surface acidic groups in **NANOCAT-G1-4**

Carbon material	**Type of acidic groups**	**Content of given acidic groups (mmol/g)**
NANOCAT-G1 (Fe@C)	N.A.[a]	0.02
NANOCAT-G2 (Fe@C-COOH)	COOH	0.53
NANOCAT-G3 (Fe@C-$(CH_2)_2$-COOH)	COOH	1.42
NANOCAT-G4 (Fe@C-Ph-SO_3H)	SO_3H	2.11

[a] see description in text

Table 3. Comparison of the catalytic activity of **NANOCAT-G4** with previously reported heterogeneous catalysts for the synthesis of 2-phenylbenzimidazole

Entry	**Catalyst**	**Reaction time**	**Yield (%)**	**Reference**
1	**NANOCAT-G4**	**50 min**	**95.0**	**This work**
2	GO	70 h	86.0	[41]
3	Graphite/p-TsOH	40 min	40.0	[40]
4	Graphite/*N*,*N*-dimethylaniline	4 h	67.0	[40]
5	Fe_3O_4 nanoparticles	45 min	80.0	[42]
6	Dowex-20 (ion-exchange resign)	12 h	85.0	[41]
7	Indion-190 (ion-exchange resign)	4 h	89.0	[48]
8	Indion-652 (ion-exchange resign)	4 h	53.0	[41]
9	Amberlite IR-120 (ion-	4 h	80.0	[41]

View Article Online
DOI: 10.1039/C8DT00677F

	exchange resign)			

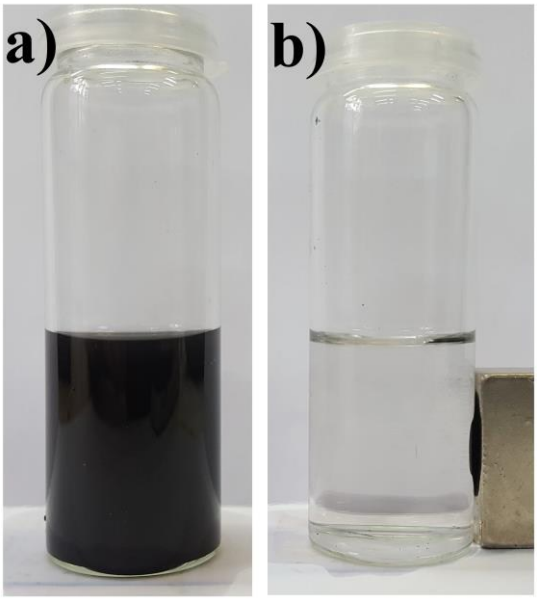

Fig. 1. (**a**) Dispersion of **NANOCAT-G4** (Fe@C-Ph-SO_3H) in ethanol (300 μg/mL) after sonication for 5 min, (**b**) magnetic response of **NANOCAT-G4** in the presence of neodymium magnet

The obtained results for the condensation of benzaldehyde and 1,2-phenylenediamine using **NANOCAT-G4** as the highly efficient magnetic nanocatalyst, prompted us to expand a list of aldehydes that may be subjected to the process. Both substituted aromatic aldehydes, as well as aliphatic and metallocene aldehydes were included in our study. The results are summarized in **Table 4**. For each entry the reaction yield was very high, i.e. between 92.5% and 97.0%. NMR and FT-IR measurements proved the formation of pure products (Figs. S3-S41 in ESI Importantly, washing of the catalyst **NANOCAT-G4** with ethanol after the reaction enabled to clean its surface and desorbed the product of the reaction. It should be also noted that the reaction yield in the case of synthesis of 2-(1-pyrenyl)benzimidazole (**7**; entry 7, **Table 4**, reaction time 45 min) was increased when the catalyst was washed with ethanol

View Article Online
DOI: 10.1039/C8DT00677F

after the reaction two more times (see details in the experimental section). Such phenomenon was most probably associated with the well-known fact, i.e. relatively strong adsorption of pyrene compounds onto carbon materials. Single washing of the catalyst was therefore sufficient for all the products (**1-13**) except 2-(1-pyrenyl)benzimidazole (**7**). The reaction time varied between 25 min and 65 min depending on the aldehyde used. For aromatic aldehydes substituted with electron donating groups (entries 2-6, **Table 4**) the reactions proceeded in a shorter time (30-40 min, 50 min in case of **6**) in comparison to the synthesis of 2-phenylbenzimidazole (**1**; 50 min). The shortest reaction time was observed in the case of the synthesis of 2-(ferrocenyl)benzimidazole (**8**; 25 min). On the other hand, for aromatic aldehydes which contained electron withdrawing groups (entries 9-11, **Table 4**), heterocyclic aldehyde (synthesis of 2-(2-pyridyl)benzimidazole, entry 11, **Table 4**) and the aliphatic aldehydes (entries 12-13, **Table 4)** the reaction time was slightly longer (55-65 min).

Table 4. Synthesis of various benzimidazoles using **NANOCAT-G4** as a nanocatalyst. Reactions conditions: aldehyde (0.4 mmol), 1,2-phenylenediamine (0.4 mmol), **NANOCAT-G4** (20 mg)[a], ethanol (7 mL), temperature: 40 °C (ultrasonic irradiation). See subsection 2.3 for experimental details

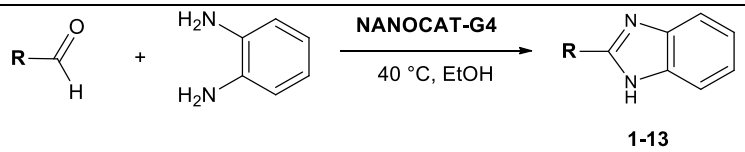

Entry	-R (aldehyde)	Product	Reaction time (min)	Yield[b] (%)
1	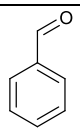	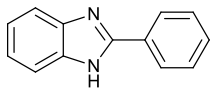 **1**	50	95.0
2	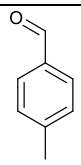	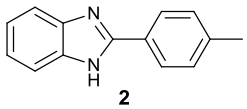 **2**	40	96.5

View Article Online
DOI: 10.1039/C8DT00677F

3	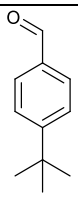	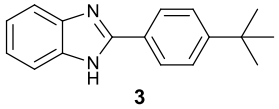 **3**	40	95.0
4	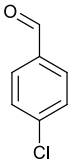	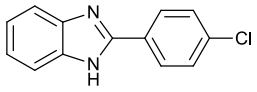 **4**	35	96.5
5	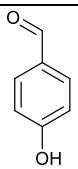	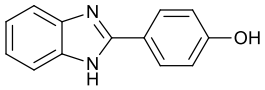 **5**	35	96.5
6	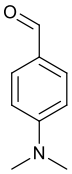	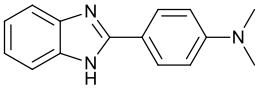 **6**	50	94.5
7	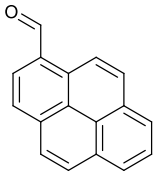	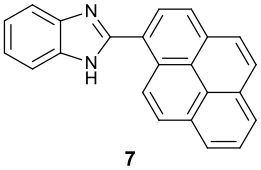 **7**	45	95.0
8	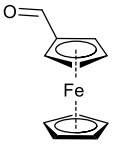	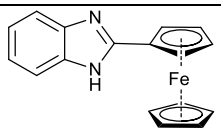 **8**	25	92.5
9	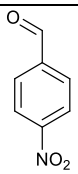	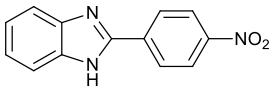 **9**	65	94.5
10	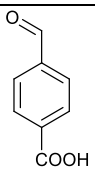	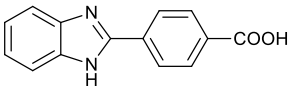 **10**	60	95.0
11	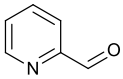	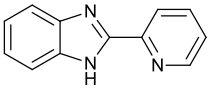 **11**	60	95.5
12	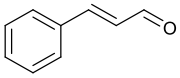	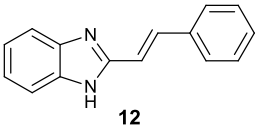 **12**	55	96.5

View Article Online
DOI: 10.1039/C8DT00677F

13	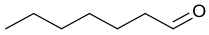	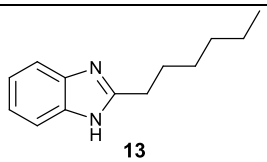 13	60	97.0

[a] for the structure of **NANOCAT-G4**, see scheme 1c
[b] isolated yields

3.2 Recyclability study

The catalyst was separated from the reaction mixture, washed with ethanol, dried in oven in 45 °C for 24 h and reused. The catalytic activity of **NANOCAT-G4** was then studied in five cycles after the first reaction (see details in subsection 2.4). The condensation of benzaldehyde and 1,2-phenylenediamine was selected as the representative process. **NANOCAT-G4** was isolated after each cycle and purified using the above-mentioned protocol. No significant difference in the reaction yield was observed for five reaction cycles (**Fig. 2**). Additionally, no changes in the FT-IR spectra were observed for **NANOCAT-G4** between the cycles (Fig. S42).

View Article Online
DOI: 10.1039/C8DT00677F

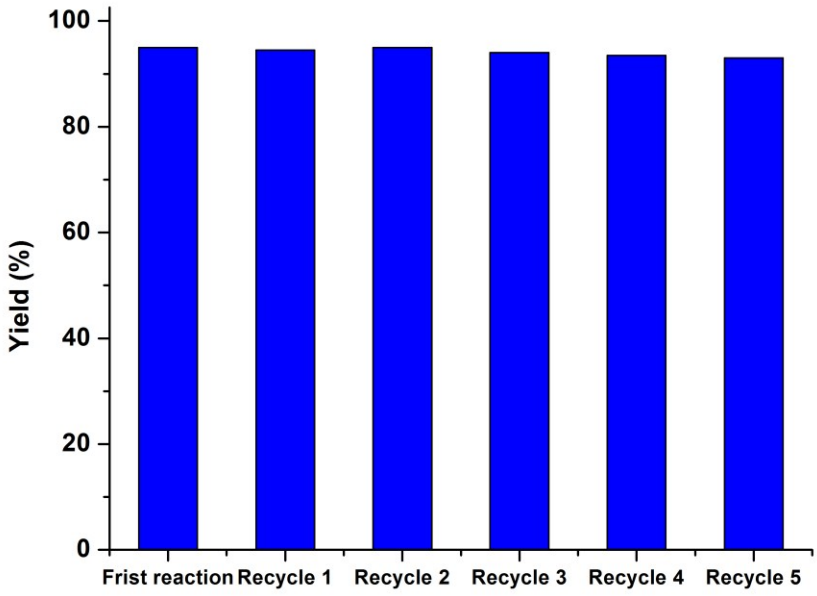

Fig. 2. Recyclability study of **NANOCAT-G4** for the synthesis of 2-phenylbenzimidazole. For the reaction scheme, see **Table 1**.

3.3 Proposed reaction mechanism

High catalytic activity of **NANOCAT-G4** was likely a result of two synergistic interface effects, namely (i) presence of the acidic groups on the surface of the **NANOCAT-G4**, and (ii) physicochemical properties of graphene coating, toward π- π process. As presented in **Fig. 3**, highly acidic sulfonyl groups protonate the oxygen atom of carbonyl moiety in the aromatic aldehyde. The electrophilicity of carbonyl carbon atom was then increased, and it facilitated the activity of the aldehydes toward the reaction with the nucleophile, i.e. 1,2-phenylenediamine. It is also reasoned that the herein developed process for the synthesis of benzimidazoles could also be facilitated by the adsorption of the reactants on the surface of CEINs during the reaction.[40]

View Article Online
DOI: 10.1039/C8DT00677F

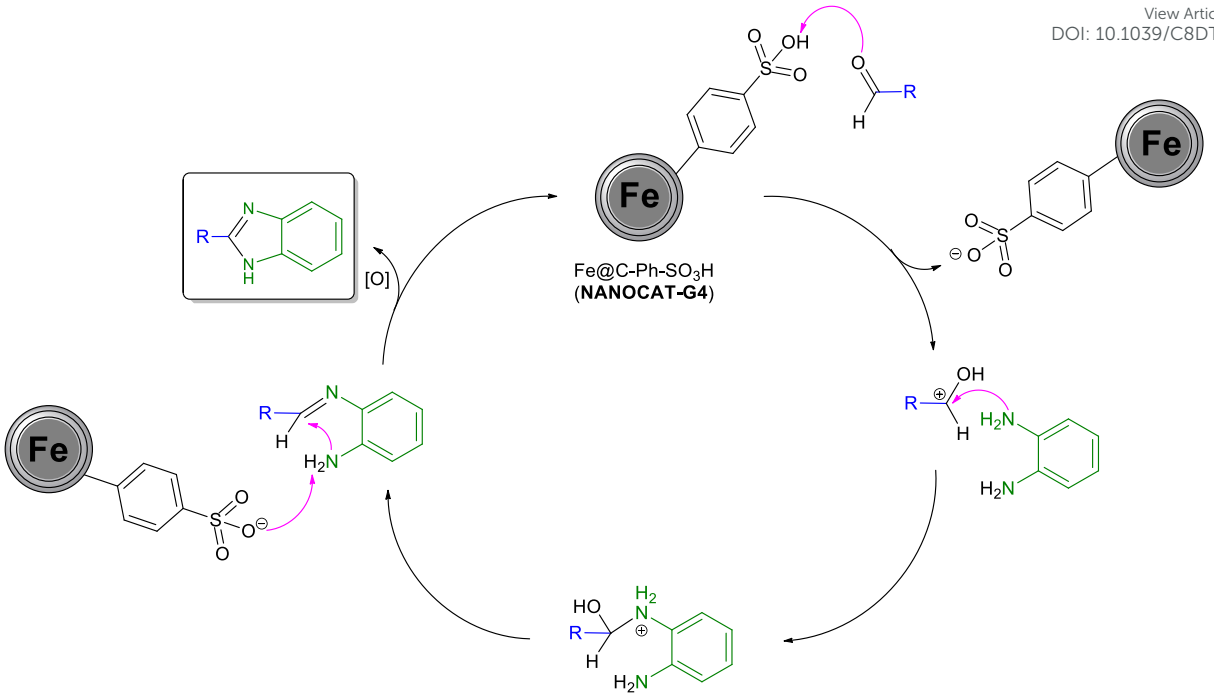

Fig. 3. Proposed reaction mechanism

4 Conclusions

The catalytic activity of carbon-encapsulated iron nanoparticles (CEINs) and CEINs functionalized with carboxyl or sulfonyl groups, in the synthesis of benzimidazoles, were examined. It was found that sulfonated CEINs (**NANOCAT-G4)** act as the very efficient and highly selective magnetic nanocatalyst. The reaction yield varied between 92.5% to 97.0%, whilst reaction time was 25-65 min, depending on the applied aldehyde. Both aliphatic, aromatic, heterocyclic and metallocene aldehydes were subjected to the reaction with 1,2-phenylenediamine. The process is simple, and the reaction occurs under mild conditions (ultrasonic irradiation, 40 °C) The nanocatalyst could be also easily separated from the reaction mixture using a permanent magnet. The recyclability studies revealed that the developed nanocatalyst retain its extraordinary activity up to six reaction cycles. By comparison to the previously reported heterogeneous catalysts for the synthesis of benzimidazoles, **NANOCAT-G4** had the best catalytic performance because of the highest

reaction yield and the shortest reaction time. Importantly, the developed method for the one-step synthesis of **NANOCAT-G4** is based on the diazotization approach, which is simple and efficient. For this carbon material both the content of the introduced organic moiety (28.0 wt%) and total acidity (2.11 mmol/g) were remarkably high. This work opens up new avenues for the development of novel magnetic nanocatalysts, as well as highly selective and efficient ways for the synthesis of benzimidazoles.

5 Acknowledgments

This work was financially supported by the National Science Center (Poland) through the grant PRELUDIUM No. 2016/21/N/ST5/00864 and Warsaw University Of Technology. Authors thanks Dr. G. Z. Żukowska for her assistance in FT-IR experiments.

6 References

1 S. Navalon, A. Dhakshinamoorthy, M. Alvaro, M. Antonietti and H. García, *Chem. Soc. Rev.*, 2017, **46**, 4501–4529.

2 C. Su and K. P. Loh, *Acc. Chem. Res.*, 2013, **46**, 2275–2285.

3 Y. Lin, J. Ren and X. Qu, *Acc. Chem. Res.*, 2014, **47**, 1097–1105.

4 V. Georgakilas, M. Otyepka, A. B. Bourlinos, V. Chandra, N. Kim, K. C. Kemp, P. Hobza, R. Zboril and K. S. Kim, *Chem. Rev.*, 2012, **112**, 6156–6214.

5 O. G. Apul, Q. Wang, Y. Zhou and T. Karanfil, *Water Res.*, 2013, **47**, 1648–1654.

6 L. Feng, S. Zhang and Z. Liu, *Nanoscale*, 2011, **3**, 1252.

7 N. Cheng, S. Stambula, D. Wang, M. N. Banis, J. Liu, A. Riese, B. Xiao, R. Li, T. K. Sham, L. M. Liu, G. A. Botton and X. Sun, *Nat. Commun.*, 2016, **7**, 1–9.

8 T. Vats, S. Dutt, R. Kumar and P. F. Siril, *Sci. Rep.*, 2016, **6**, 1–11.

9 S. Ghasemi, S. R. Hosseini, S. Nabipour and P. Asen, *Int. J. Hydrogen Energy*, 2015,

View Article Online
DOI: 10.1039/C8DT00677F

40, 16184–16191.

10 A. Schaetz, M. Zeltner and W. J. Stark, *ACS Catal.*, 2012, **2**, 1267–1284.

11 P. Wang, Y. Bai, H. Xiao, S. Tian, Z. Zhang, Y. Wu, H. Xie, G. Yang, Y. Han and Y. Tan, *Catal. Commun.*, 2016, **75**, 92–97.

12 X. Pan and X. Bao, *Acc. Chem. Res.*, 2011, **44**, 553–562.

13 B. Garg and Y. Ling, *Green Mater.*, 2014, **1**, 47–61.

14 A. M. Dimiev, L. B. Alemany and J. M. Tour, *ACS Nano*, 2013, **7**, 576–588.

15 T. Ji, Y. Hua, M. Sun and N. Ma, *Carbon*, 2013, **54**, 412–418.

16 G. Modugno, C. Ménard-Moyon, M. Prato and A. Bianco, *Br. J. Pharmacol.*, 2015, **172**, 975–991.

17 J. K. Park, J. Jung, P. Subramaniam, B. P. Shah, C. Kim, J. K. Lee, J. H. Cho, C. Lee and K. B. Lee, *Small*, 2011, **7**, 1647–1652.

18 E. K. Lim, T. Kim, S. Paik, S. Haam, Y. M. Huh and K. Lee, *Chem. Rev.*, 2015, **115**, 327–394.

19 T. Pasinszki, M. Krebsz, L. Kótai, I. E. Sajó, Z. Homonnay, E. Kuzmann, L. F. Kiss, T. Váczi and I. Kovács, *J. Mater. Sci.*, 2015, **50**, 7353–7363.

20 L. Kótai, T. Pasinszki, Z. Czégény and S. Bálint, *Eur. Chem. Bull.*, 2012, **1**, 398–400.

21 R. Fuhrer, I. K. Herrmann, E. K. Athanassiou, R. N. Grass and W. J. Stark, *Langmuir*, 2011, **27**, 1924–1929.

22 M. Rossier, F. M. Koehler, E. K. Athanassiou, R. N. Grass, B. Aeschlimann, D. Günther and W. J. Stark, *J. Mater. Chem.*, 2009, **19**, 8239.

23 X. Ling, J. Li, W. Zhu, Y. Zhu, X. Sun, J. Shen, W. Han and L. Wang, *Chemosphere*, 2012, **87**, 655–660.

24 H. H. Tseng, J. G. Su and C. Liang, *J. Hazard. Mater.*, 2011, **192**, 500–506.

25 M. Bystrzejewski, O. Łabedź, W. Kaszuwara, A. Huczko and H. Lange, *Powder*

View Article Online
DOI: 10.1039/C8DT00677F

Technol., 2013, **246**, 70–15.

26 M. Fronczak, O. Łabędź, W. Kaszuwara and M. Bystrzejewski, *J. Mater. Sci.*, 2017, **53**, 3805–3816.

27 M. Bystrzejewski, A. Huczko and H. Lange, *Sensors Actuators, B Chem.*, 2005, **109**, 81–85.

28 R. N. Grass, E. K. Athanassiou and W. J. Stark, *Angew. Chemie - Int. Ed.*, 2007, **46**, 4909–4912.

29 G. Wang, G. Wan and C. Hao, *Mod. Phys. Lett. B*, 2009, **23**, 2149–2153.

30 M. Bystrzejewski, R. Klingeler, T. Gemming, B. Büchner and M. H. Rümmeli, *Nanotechnology*, 2011, **22**, 315606 (10pp).

31 M. Poplawska, M. Bystrzejewski, I. P. Grudzinski, M. A. Cywinska, J. Ostapko and A. Cieszanowski, *Carbon*, 2014, **74**, 180–194.

32 Y. Ma, B. Yue, L. Yu, X. Wang, Z. Hu, Y. Fan, Y. Chen, W. Lin, Y. Lu and J. Hu, *J. Phys. Chem. C*, 2008, **112**, 472–475.

33 A. Kasprzak, M. Poplawska, M. Bystrzejewski and I. P. Grudzinski, *J. Mater. Chem. B*, 2016, **4**, 5593–5607.

34 A. Kasprzak, A. M. Nowicka, J. P. Sek, M. Fronczak, M. Bystrzejewski, M. Koszytkowska-Stawinska and M. Poplawska, *Dalt. Trans.*, 2018, **47**, 30.

35 A. Kasprzak, M. Bystrzejewski, M. Koszytkowska-Stawinska and M. Poplawska, *Green Chem.*, 2017, **19**, 3510–3514.

36 M. Poplawska, G. Z. Zukowska, S. Cudziło and M. Bystrzejewski, *Carbon*, 2010, **48**, 1318–1320.

37 A. Schätz, T. R. Long, R. N. Grass, W. J. Stark, P. R. Hanson and O. Reiser, *Adv. Funct. Mater.*, 2010, **20**, 4323–4328.

38 M. Keller, V. Collière, O. Reiser, A. M. Caminade, J. P. Majoral and A. Ouali, *Angew.*

View Article Online
DOI: 10.1039/C8DT00677F

Chemie - Int. Ed., 2013, **52**, 3626–3629.

39 J. Velík, V. Baliharová, J. Fink-Gremmels, S. Bull, J. Lamka and L. Skálová, *Res. Vet. Sci.*, 2004, **76**, 95–108.

40 H. Sharghi, S. Mohammad and H. Tabaei, *J. Heterocycl. Chem.*, 2008, **45**, 1293.

41 K. B. Dhopte, R. S. Zambare, A. V. Patwardhan and P. R. Nemade, *RSC Adv.*, 2016, **6**, 8164–8172.

42 B. Kumar, K. Smita, L. Cumbal and A. Debut, *J. Saudi Chem. Soc.*, 2014, **18**, 364–369.

43 Z. Li, A. Zhu and J. Yang, *J. Heterocycl. Chem.*, 2012, **49**, 1458–1461.

44 V. Zlateski, R. Fuhrer, F. M. Koehler, S. Wharry, M. Zeltner, W. J. Stark, T. S. Moody and R. N. Grass, *Bioconjug. Chem.*, 2014, **25**, 677–684.

45 A. M. Nowicka, A. Kowalczyk, M. Bystrzejewski, M. Donten and Z. Stojek, *Electrochem. Commun.*, 2012, **20**, 4–6.

46 P. S. J. Canning, K. McCrudden, H. Maskill and B. Sexton, *J. Chem. Soc. Perkin Trans. 2*, 1999, 2735–2740.

47 I. P. Grudzinski, M. Bystrzejewski, M. A. Cywinska, A. Kosmider, M. Poplawska, A. Cieszanowski and A. Ostrowska, *J. Nanoparticle Res.*, 2013, **16**, 1835.

48 V. S. Padalkar, V. D. Gupta, K. R. Phatangare, V. S. Patil, P. G. Umape and N. Sekar, *Green Chem. Lett. Rev.*, 2012, **5**, 139–145.

View Article Online
DOI: 10.1039/C8DT00677F

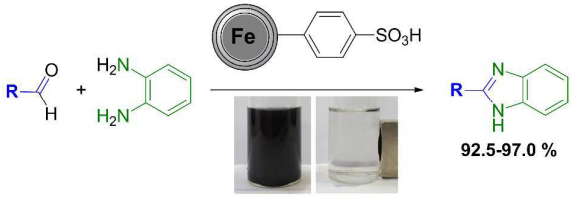

Various benzimidazoles were obtained applying sulfonated carbon-encapsulated iron nanoparticles as the nanocatalyst.